

### 3.4 THz heterodyne receiver using a hot electron bolometer and a distributed feedback quantum cascade laser

P. Khosropanah,<sup>1</sup> W. Zhang,<sup>1,2</sup> J. N. Hovenier,<sup>3</sup> J. R. Gao,<sup>1,3,a)</sup> T. M. Klapwijk,<sup>3</sup>  
M. I. Amanti,<sup>4</sup> G. Scalari,<sup>4</sup> and J. Faist<sup>4</sup>

<sup>1</sup>*SRON Netherlands Institute for Space Research, Landleven 12, 9747AD Groningen, The Netherlands*

<sup>2</sup>*Purple Mountain Observatory (PMO), National Astronomical Observatories of China (NAOC), Chinese Academy of Sciences, 2 West Beijing Road, Nanjing, JiangSu 210008, China*

<sup>3</sup>*Kavli Institute of Nanoscience, Delft University of Technology, Lorentzweg 1, 2628 CJ Delft, The Netherlands*

<sup>4</sup>*Institute of Quantum Electronics, ETH-Zürich, CH-8096 Zürich, Switzerland*

(Received 10 July 2008; accepted 10 October 2008; published online 2 December 2008)

We report a heterodyne receiver using a superconducting NbN hot electron bolometer (HEB) integrated with a tight winding spiral antenna as mixer and a distributed feedback (DFB) terahertz quantum cascade laser (QCL) operating at 3.42 THz as local oscillator. The aim is to demonstrate the readiness of both devices for the detection of OH lines at 3.5 THz in a real instrument. We show that the improved single-spot beam of the terahertz QCL can easily pump the HEB mixer. We measured a double sideband receiver noise temperature of 2100 K at the optimum local oscillator power of 290 nW. This noise temperature can be further reduced to 1100 K if we correct the loss due to the use of an uncoated lens, and the losses of the window and the air. Therefore, the combination of a HEB and such a DFB QCL can in principle be used to detect an OH line at 3.5 THz. However, a high input power of several watts, which is needed to operate the QCL in a liquid-helium cryostat, poses a big challenge to the receiver stability. © 2008 American Institute of Physics.

[DOI: [10.1063/1.3032354](https://doi.org/10.1063/1.3032354)]

## I. INTRODUCTION

Problems related to the earth's atmosphere such as global warming and ozone destruction can be monitored and better understood by observations in the far infrared. This frequency band holds the most important spectral signatures of the relevant molecules. Among these, the hydroxyl (OH) radical has been identified as a crucial probe<sup>1</sup> and has emission lines at frequencies such as 1.8, 2.5, and 3.5 THz. OH is the dominant oxidizing chemical in the atmosphere. It destroys most air pollutants and many gases involved in ozone depletion and the greenhouse effect. To detect them and resolve the line spectrum, it is desirable to have a sensitive heterodyne receiver operated in a balloon-borne or a space-borne observatory. The key components of such a receiver are a mixer and a terahertz coherent source as local oscillator (LO). Several space-borne or balloon-borne instruments have been constructed to detect OH lines. For example, NASA's Earth Observing System Microwave Limb Sounder (EOS-MLS),<sup>2</sup> based on a room-temperature Schottky diode as mixer and an optically pumped gas laser as LO,<sup>3</sup> is now operated to detect an OH line at 2.5 THz. Terahertz and submillimeter Limb Sounder (TELIS) is a three-channel balloon-borne heterodyne spectrometer for atmospheric research.<sup>4</sup> The 1.8 THz channel, based on a superconducting NbN hot electron bolometer (HEB) mixer and a solid state multiplier LO unit, will focus on the OH lines at this frequency.

Figure 1 shows a predicted spectrum of OH lines close to 3.5 THz. The OH line at 3.551 THz is ideal for monitoring and retrieval.<sup>5</sup> This is the brightest OH emission feature and is well isolated from other molecular lines, decreasing the likelihood of spectral confusion. However, OH lines at 3.5 THz have never been studied by high-resolution heterodyne spectrometer due to lack of suitable LOs at this particular frequency. Solid state LOs based on multipliers have been demonstrated up to 2 THz, but are unlikely to generate sufficient output power at such a high frequency. Optically pumped gas lasers can be operated at a high frequency but have no strong lasing lines very close to 3.5 THz OH lines.

Terahertz quantum cascade lasers (QCLs) (Refs. 6 and 7) are an appealing choice as a LO for this specific frequency

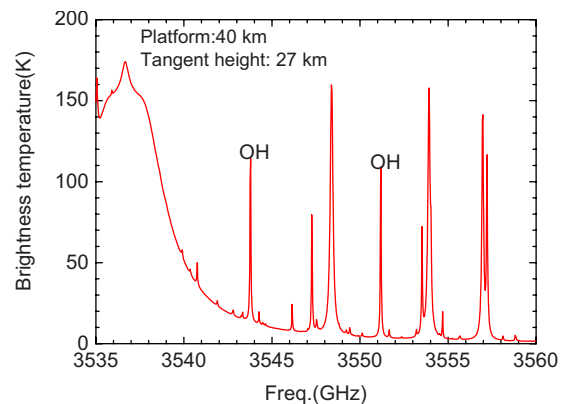


FIG. 1. (Color online) Simulated emission spectrum of OH lines in the atmosphere for an instrument at 40 km in limb geometry. The tangent height is 27 km.

<sup>a)</sup>Author to whom correspondence should be addressed. Electronic mail: [j.r.gao@tudelft.nl](mailto:j.r.gao@tudelft.nl).

because of their compactness, high output power, linear polarization, narrow linewidth, and frequency/phase locking capability.<sup>8,9</sup> Terahertz QCLs have been successfully demonstrated as LOs in the laboratory using either a double-metal waveguide<sup>10</sup> or a surface-plasmon waveguide structure.<sup>11,12</sup> They all employ a Fabry-Pérot cavity which can achieve a single-mode lasing but is unable to control the operating frequency precisely, e.g., not within an accuracy of a few gigahertz. Therefore, for the detection of the OH line at 3.551 THz, an additional mode control mechanism should be introduced to terahertz QCLs. Currently a distributed feedback (DFB) structure is known to achieve the single-mode operation at a designed frequency.<sup>13</sup>

Here we report measurements of a heterodyne receiver that combines a superconducting NbN HEB mixer and a terahertz DFB QCL at 3.42 THz, and demonstrate low noise performance of the receiver. To overcome the problem caused by high input power to the QCL, which results in instability of LO power from the QCL, we applied a different characterization method for the receiver sensitivity.<sup>14</sup>

## II. TERAHERTZ DFB QCLS

The QCL used in our experiment is developed by the group at ETH-Zürich, Switzerland. The active region, based on a bound-to-continuum design,<sup>15</sup> is a GaAs/AlGaAs materials system on a semi-insulating GaAs substrate grown by molecular beam epitaxy. The DFB structure is based on strongly coupled surface grating fabricated with wet chemical etching and metal coverage.<sup>16</sup> All side “facets” of the laser ridge are fully covered by the metal layer. The periodicity ( $\Lambda$ ) of the first-order Bragg gratings determines the emission frequency as follows:  $\Lambda = \lambda_{wg}/2n_g$ , where  $\lambda_{wg}$  and  $n_g$  are the designed wavelength and effective refractive index, respectively. The lasing spectrum of a terahertz DFB QCL with a ridge width of 200  $\mu\text{m}$  and a length of 1.25 mm has been measured using a Fourier transform spectrometer (FTS). Results show a single-mode or monochromatic emission at 3.42 THz within a resolution of  $\sim 0.7$  GHz. This QCL is appropriate for demonstrating a receiver for the 3.551 THz OH line because the difference in frequency is so small that it makes virtually no difference in the sensitivity. The input dc power of the terahertz DFB QCL is about 5 W when operated in continuous wave (cw) mode. The QCL is mounted in a liquid-helium (L-He) vacuum cryostat and the high required input power makes the temperature stabilization difficult, resulting in output power fluctuations.

## III. HEB MIXER

The HEB mixer used is shown in Fig. 2. It consists of a 2  $\mu\text{m}$  wide, 0.2  $\mu\text{m}$  long, and 5.5 nm thick NbN bridge on a highly resistive Si substrate covered by a native oxide.<sup>17,18</sup> The bridge is connected to the antenna by NbTiN (10 nm)/Au (50 nm) bilayer contact pads. The antenna is an on-chip spiral made of a 170 nm thick Au layer. It has a tight winding design with an inner diameter of 6.6  $\mu\text{m}$  close to the NbN bridge (see the inset of Fig. 2). Based on the study in Ref. 19 and our previous results using a design with a diameter of 15  $\mu\text{m}$ , an expected upper cutoff frequency of

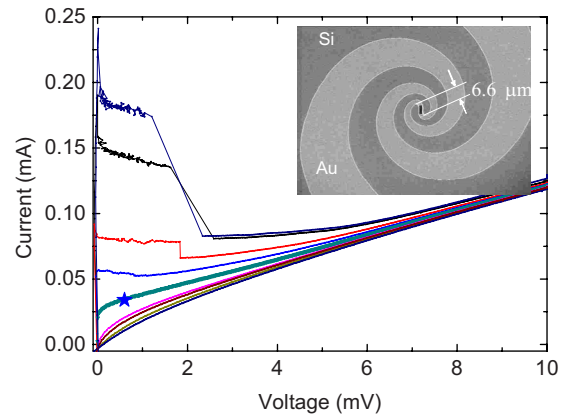


FIG. 2. (Color online) A set of current-voltage curves of a NbN HEB mixer at 4.2 K at different LO powers from a 3.42 THz DFB QCL, where the center of the optimum operating region is indicated by a star. The inset shows a scanning electron micrograph of a HEB integrated with a spiral antenna (inner diameter is 6.6  $\mu\text{m}$ ).

this antenna is about 6 THz. The HEB has a room-temperature resistance of 80  $\Omega$  and a critical current of 275  $\mu\text{A}$  at 4.2 K. This HEB has demonstrated an extremely low (double sideband (DSB)) receiver noise temperature of 1300 K at 4.3 THz using a Far Infrared (FIR) gas laser as LO and a vacuum measurement setup for hot/cold calibration loads.<sup>14</sup>

## IV. HETERODYNE MEASUREMENT SETUP

Figure 3 shows a schematic view of the heterodyne measurement setup. We use two L-He vacuum cryostats (Infrared Laboratories), in which the QCL and the HEB are mounted separately. A large cryostat with 8.3 l of L-He capacity was used for the QCL. This provides about an hour of holding time when the laser is operated as a LO in cw mode and with an input power of 5 W. However, during the optical alignment of the setup, the QCL is operated in a pulsed mode, which reduces the dc input power considerably. The output power of the QCL was coupled to the HEB antenna using a

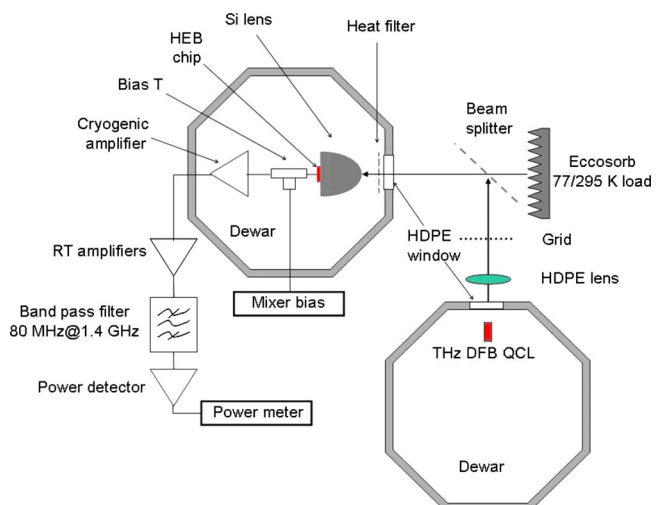


FIG. 3. (Color online) Schematic view of the heterodyne measurement setup, where a NbN HEB mixer and a terahertz DFB QCL are separately mounted in two vacuum L-He4 cryostats.

standard quasioptical technique. The Si chip with the HEB was glued to the backside of an elliptical Si lens without antireflection coating, placed in a metal mixer block, and thermally anchored to the 4.2 K cold plate of the HEB cryostat. The beam from the QCL passed through a high-density polyethylene (HDPE) window of the QCL cryostat and was collimated with a HDPE lens ( $f=50$  mm). The QCL emission was combined with the radiation of 295 K (hot)/77 K (cold) load by a 3.5  $\mu\text{m}$  thick Mylar beam splitter. The signals passed through an HDPE vacuum window (1 mm thick) and a QMC low-pass (or heat) filter,<sup>20</sup> mounted on the 4 K shield of the HEB cryostat. A computer-controlled wire grid was inserted into the LO path between the HDPE lens and the beam splitter in order to regulate the amount of LO power coupling to the HEB.

The intermediate frequency (IF) signal, resulting from the mixing of the LO and the hot/cold load signals, is amplified first using a cryogenic low noise amplifier operated at 4.2 K and then by room-temperature amplifiers. This signal is filtered at 1.4 GHz in a band of 80 MHz. The entire IF chain has a gain of about 80 dB and a noise temperature of 7 K.

## V. MEASUREMENT RESULTS

### A. Beam patterns of the DFB QCL

The terahertz DFB QCL used in this work is expected to have a diffraction-limited single-spot beam, which is reasonable for coupling the radiation to a mixer. However, in practice, the beam contains highly dense interference fringes in the far-field pattern<sup>21</sup> [see Fig. 4(a)] although the envelope of the beam is determined by the effective area of the facet and the wavelength and thus is diffraction limited. The interference fringes from the same device were also observed in a different beam-measurement setup (not shown here) at ETH-Zürich.

Despite of an output power of 3 mW in cw mode, it was not possible to pump the HEB mixer that requires only 290 nW of LO power (at HEB). In this case, the QCL and HEB cryostats were placed directly face to face (no beam splitter was used) and we tried HDPE lenses with different focal distances in between to collimate the beam of the QCL. Although a HDPE lens has 1.5 dB loss at this frequency, the reduction in the power is negligible in comparison with what we gain by collimating the beam. We confirmed the 3 mW output power of the QCL by replacing the HEB mixer by a room-temperature pyroelectric detector at the exact same focal point. The total optical loss (including the air, cryostat windows, low-pass filter, Si lens, and antenna of circular polarization responding to the linear polarized radiation) is 8.8 dB. Thus, the optical loss is unable to account for a huge difference ( $\sim 10^4$ ) between the output power of the QCL and the power needed for pumping the HEB.

The physical reason for why the HEB mixer cannot be pumped by this QCL is the highly dense interference fringes in the far-field beam pattern [see Fig. 4(a)]. More precisely, this is due to a combination of the beam with varying phase front and an antenna coupled HEB mixer, which is a power-law coherent detector. By considering a simplified case

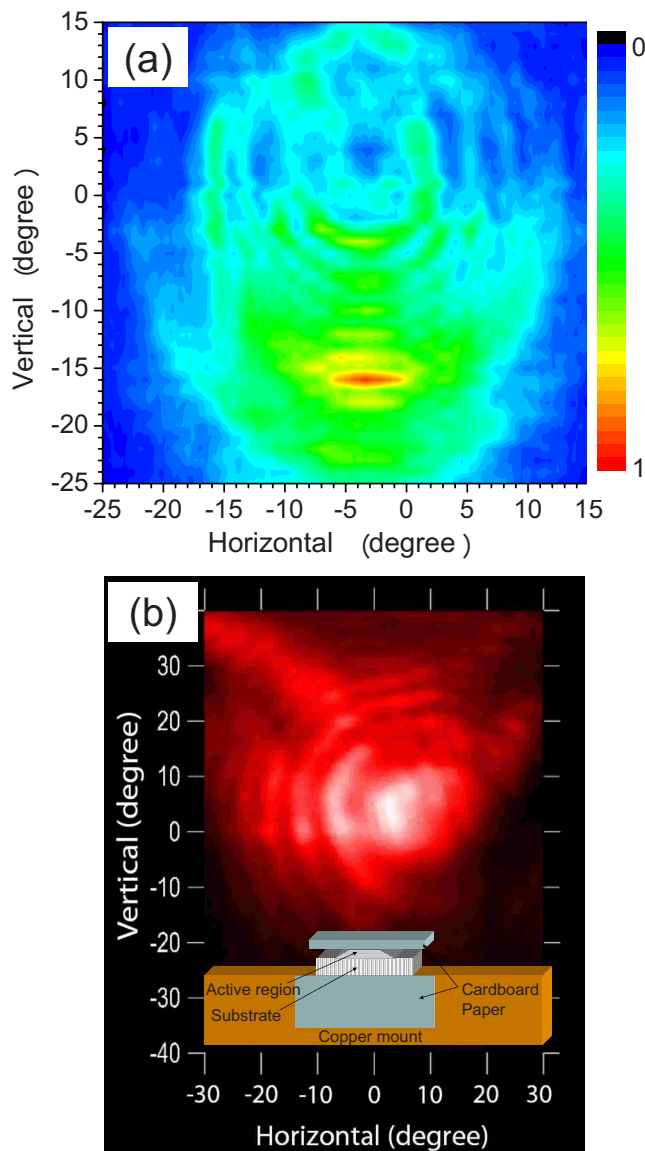


FIG. 4. (Color online) Measured two dimensional far-field beam patterns of two very similar terahertz DFB QCLs. Original beam pattern with highly dense interference fringes and a minimum in the laser pointing direction for one DFB QCL in (a); improved beam pattern after adding cardboard papers as terahertz absorbers on top of the laser bar and also on the Cu metal mount underneath the substrate for another DFB QCL in (b), where the inset shows a schematic drawing of the QCL. From the top, one sees a cardboard paper, the active region (laser bar), the substrate, and the Cu mount covered with a cardboard paper.

where two radiation beams with the same amplitude but in opposite phases are coupled into the HEB mixer via a phase sensitive antenna, the total power detected by the HEB mixer in this case is simply zero. When the beam with the highly dense interference fringes is coupled into a HEB mixer, it behaves in a similar way as many beams with equal amplitude but different phases. Therefore the HEB mixer is unable to see the total radiation power from such a beam, but only a relatively small fraction of it.

To reduce or eliminate the interference fringes, we have introduced cardboard papers as terahertz absorbers on top of the laser bar and also on the Cu metal mount underneath the substrate<sup>22</sup> [see the inset of Fig. 4(b)]. This was achieved in a very similar DFB QCL. Now the far-field beam pattern

shows trends toward a single-spot beam, as illustrated in Fig. 4(b). The physical origin of these effects on the beam shape is still under study. It is likely that, due to the absorber, the parasitic radiation is decoupled from radiation emitted from the front facet. One of the parasitic radiation sources can be due to the antenna effect as found in metal-metal waveguide QCLs.<sup>23,24</sup> Detailed discussions on this issue are beyond the scope of this paper.

The DFB QCL with an improved beam pattern emits a maximum output power of 2 mW in cw mode, measured at a 10–20 K QCL bath temperature. We notice that this output power is lower than the power ( $\sim 3$  mW) before adding the absorbers. Despite of reduced total output power, the single-spot beam now allows for pumping a NbN HEB mixer sufficiently. The laser can easily overpump the HEB when they are placed face to face with a HDPE lens in between to collimate the beam and even when using a thin  $3.5 \mu\text{m}$  Mylar beam splitter in the heterodyne setup as shown in Fig. 3.

## B. Heterodyne results

We measured the hot and cold receiver output noise powers,  $P_{\text{out,hot}}$  and  $P_{\text{out,cold}}$ . We used the  $Y$ -factor ( $Y = P_{\text{out,hot}}/P_{\text{out,cold}}$ ) method to obtain the DSB receiver noise temperature ( $T_{N,\text{rec}}$ ), which is

$$T_{N,\text{rec}} = \frac{T_{\text{eff,hot}} - Y T_{\text{eff,cold}}}{Y - 1},$$

where  $T_{\text{eff,hot}}$  and  $T_{\text{eff,cold}}$  are the equivalent temperatures of a blackbody at 295 and 77 K, respectively. Using the Callen–Welton definition,  $T_{\text{eff,hot}}$  and  $T_{\text{eff,cold}}$  become 302.7 and 104.6 K at 3.42 THz.<sup>25</sup>

Figure 2 shows a typical set of current-voltage ( $I$ - $V$ ) curves of the HEB pumped by the QCL from zero power to fully pumped power levels. The best sensitivity is obtained around the region indicated with a star where the LO pump power is about 290 nW, the bias voltage is 0.6 mV, and the bias current is  $30 \mu\text{A}$ .

Due to LO power drifting, we were unable to obtain reliable sensitivity data using a standard method for HEB characterization, in which LO power is fixed but the bias voltage is varied. We now apply a different characterization method as introduced in Ref. 14 to measure the DSB receiver noise temperature. In this case we measure the receiver output noise power as a function of bias current, under a fixed bias voltage, while continuously varying the LO power using the wire grid. Note that the current exactly follows the change in LO power. This moves the bias point vertically on the  $I$ - $V$  curves from the fully pumped to the unpumped region or vice versa. Two data sets were recorded.  $P_{\text{out,hot}}(I)$  corresponds to the hot load and the other,  $P_{\text{out,cold}}(I)$ , corresponds to the cold load. The  $Y$ -factor was obtained by using  $Y(I) = P_{\text{out,hot}}(I)/P_{\text{out,cold}}(I)$  at exactly the same current for a fixed voltage. Figure 5 shows the measured receiver output noise power data,  $P_{\text{out,hot}}(I)$  and  $P_{\text{out,cold}}(I)$ , as a function of current at several bias voltages. By fitting each noise power data set with a polynomial, we obtained  $P_{\text{out,hot}}-I$  and  $P_{\text{out,cold}}-I$  curves and derived the DSB receiver noise temperature as a function of current at different voltages.

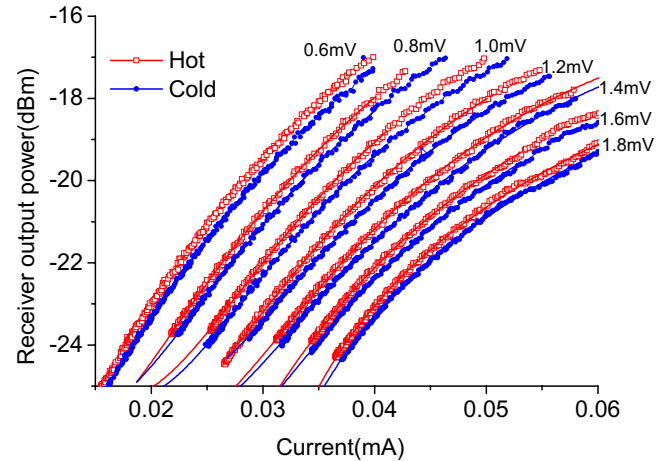


FIG. 5. (Color online) Receiver output noise power of a HEB mixer as a function of bias current for different bias voltages from 0.6 to 1.8 mV. The current directly follows the change in LO power. The red data points and curves correspond to the hot load, while the blue ones show the cold load.

The lowest receiver noise temperatures are found in the data taken at a bias voltage of 0.6 mV. The  $T_{N,\text{rec}}$  versus current, together with measured output noise power data and fitted curves, is shown in Fig. 6. The lowest  $T_{N,\text{rec}}$  was  $2100 \pm 50$  K and occurred at a bias current of  $30 \mu\text{A}$ . In fact, the ultimate receiver noise temperature could be a factor of 2 lower if we take various losses into account, including those from Si lens and vacuum window, and those due to water absorption in the air. A receiver noise temperature of 1100 K is expected at this frequency if we use an antireflection coated Si lens ( $\sim 1$  dB reflection loss) and if we perform the measurement in a vacuum hot/cold setup<sup>14</sup> (thereby eliminating 1.5 dB cryostat window loss and 0.3 dB air loss at this frequency). We emphasize that here we now established a noise temperature of a HEB receiver at a frequency in the vicinity of the 3.5 THz OH line. Furthermore, the measured receiver noise temperature at 3.42 THz is in good agreement with what can be extrapolated based on the sensitivities at 4.3 THz (Ref. 14) and at 2.8 THz,<sup>12</sup> which takes also the different losses into account.

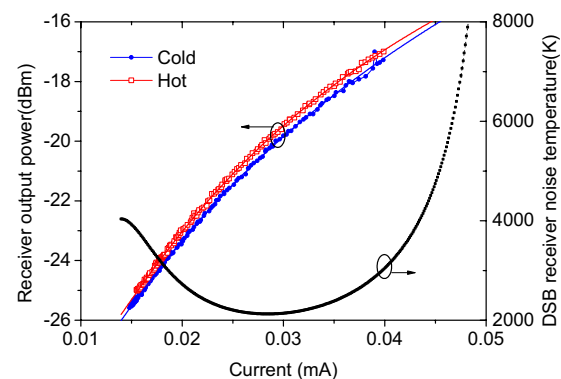


FIG. 6. (Color online) Measured receiver output noise powers of a HEB mixer at the optimum bias voltage of 0.6 mV (dots) and the polynomial fits (lines) to hot and cold powers as a function of the bias current of the HEB, which follows the change in the LO power (left axis). The resulting DSB receiver noise temperature curve as a function of the bias current of the HEB is also shown (right axis).

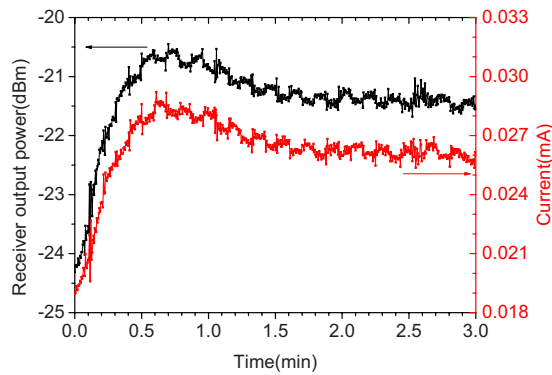


FIG. 7. (Color online) Measured receiver output noise power (left axis) and bias current of the HEB (right axis) as functions of time over the period of 3 min after turning on the terahertz DFB QCL and heating up. The small periodic jumps in both power and current curves are due to switching between hot and cold loads, which is done manually. The jumps in power reflect a heterodyne response as well as a direct detection effect, while the jumps in current curves reflect a direct detection effect.

We now turn to the issue of varying LO power and thus the instability of the receiver. As reported earlier, a terahertz QCL can offer an extremely stable output power.<sup>10</sup> However, the QCL used in this work requires about 5 W dc input power when it is operated in cw mode. The QCL was mounted on a metal holder located directly on the cold plate of the L-He cryostat. Whenever dc power was applied to the laser, the temperature monitored at the metal holder, and thus the temperature of the laser, began to increase. The laser eventually reached an operating region where the temperature became relatively stable but still drifted. As a consequence, the output power of the QCL showed a quick decrease and slow drift. Variable LO power affects the overall receiver stability. To demonstrate this instability, we simultaneously measured the receiver output noise power and bias current as functions of time over a period of 3 min immediately after turning the QCL on. As shown in Fig. 7, the receiver output noise power as well as the HEB current increased dramatically while QCL warmed up until the temperature of terahertz DFB QCL stabilized in about 1.5 min. After that the receiver output noise power and bias current drifted due to the instability of QCL output power. We also mention that because of the high input power of the laser in cw mode, the effective holding time of the QCL cryostat is about an hour,<sup>26</sup> which allows performing of heterodyne measurements, but is obviously too short for a practical instrument.

In the same experiment, we also demonstrate the effect of direct detection in the HEB due to wideband hot/cold radiation.<sup>27</sup> Because of a combination of our tight winding spiral antenna, which has a wide rf bandwidth, and the relatively small HEB, which requires low operating LO power, the amount of power from the hot and cold loads coupled into the HEB is no longer negligible in comparison with the LO power. As suggested in the curve in Fig. 7, there are additional small periodic jumps during switching between hot and cold loads. In this case a change of  $\sim 0.5 \mu\text{A}$  in the HEB bias current was observed, indicating an evident direct detection. In principle, such a direct detection effect can be eliminated by adding a narrow bandpass filter between the

mixer and hot/cold load. In practice, because we are using a different characterization method to determine the  $Y$ -factor (shown in Figs. 5 and 6), the obtained receiver noise temperature is not affected by the direct detection effect in our measurements. We note that the jumps in power in Fig. 7 reflect a heterodyne response as well as a direct detection effect.

## VI. CONCLUSIONS

In summary, we have characterized a heterodyne receiver using a HEB mixer and a terahertz DFB QCL emitting at 3.42 THz as LO in order to demonstrate a system for the detection of the OH line at 3.5 THz. We have shown that the far-field beam pattern of a terahertz DFB QCL after introducing the absorbers around the laser becomes a single-spot beam, which enables the QCL to pump a HEB mixer easily in the heterodyne setup even with a thin  $3.5 \mu\text{m}$  Mylar beam splitter. We obtained a DSB receiver noise temperature of 2100 K at 3.42 THz. The sensitivity can be reduced to 1100 K if a coated Si lens and vacuum hot/cold setup are used. These values have established a high heterodyne sensitivity in the vicinity of 3.5 THz OH line. Furthermore, the expected receiver noise temperature at this frequency indirectly confirms that the terahertz DFB QCL has a pure single-mode emission line. The reason to address this issue is that due to a limited resolution of the FTS, the measured spectrum alone is unable to confirm whether the lasing is truly single mode although it is expected. However, we find that the high input power needed to operate the QCL results in receiver instability, making measurements other than the  $Y$ -factor, including a spectroscopic measurement,<sup>28</sup> impossible.

Our goal was to realize a practical heterodyne receiver for the detection of the 3.5 THz OH line. Due to the limited availability of dry cryocoolers and electrical power for both space-based<sup>29</sup> and airborne missions,<sup>4,30</sup> we foresee several technical challenges with regard to the use of terahertz QCLs as LOs. First, the input dc power has to be far below 100 mW if it is operated around 5–10 K. An alternative is to have a terahertz QCL operated at a relatively high temperature, e.g., 70 K or higher, where the required input power is moderately reduced to as much as  $\sim 1 \text{ W}$ .<sup>29</sup> Lower dc input power<sup>31</sup> and higher operating temperature<sup>32</sup> terahertz QCLs have been demonstrated in the literature. Another key step toward realizing terahertz QCL LOs is the development of frequency or phase locking techniques. A usual way to stabilize a LO is to lock the terahertz line to a reference signal upconverted from a microwave source. However, due to lack of solid state reference sources at such a high frequency, different phase locking methods should be explored.

## ACKNOWLEDGMENTS

We acknowledge Sheng-Cai Shi at Purple Mountain Observatory, Nanjing, China, for supporting this joint research project, X. Gu and S. Paprotskiy for performing the beam measurements, M. Hajenius for fabricating the NbN HEB, and A. de Lange for providing a simulated spectrum for OH lines at 3.5 THz. The work was supported partly by China

Exchange Programme, which is the framework of the scientific cooperation between the Netherlands and P. R. China, and is executed by KNAW and CAS.

- <sup>1</sup>R. G. Prinn, J. Huang, R. F. Weiss, D. M. Cunnold, P. J. Fraser, P. G. Simmonds, A. McCulloch, C. Harth, P. Salameh, S. O'Doherty, R. H. J. Wang, L. Porter, and B. R. Miller, *Science* **292**, 1882 (2001).
- <sup>2</sup>M. C. Gaidis, H. M. Pickett, C. D. Smith, S. C. Martin, R. P. Smith, and P. H. Siegel, *IEEE Trans. Microwave Theory Tech.* **48**, 733 (2000).
- <sup>3</sup>E. R. Mueller, R. Henschke, W. E. Robotham, Jr., L. A. Newman, L. M. Laughman, R. A. Hart, J. Kennedy, and H. M. Pickett, *Appl. Opt.* **46**, 4907 (2007).
- <sup>4</sup>P. L. Yagoubov, R. W. M. Hoogeveen, A. M. Maurellis, U. Mair, M. Krocka, G. Wagner, M. Birk, H.-W. Hübers, H. Richter, A. Semenov, G. Gol'tsman, B. Voronov, V. Koshelets, S. Shitov, B. Ellison, B. Kerridge, D. Matheson, B. Alderman, M. Harman, R. Siddans, and J. Reburn, Proceedings of 14th International Symposium on Space Terahertz Technology, Tucson, Arizona, 22–24 April 2003 (unpublished), pp. 204–214.
- <sup>5</sup>A. de Lange, "TELIS and OH," SRON Internal Report, 2005.
- <sup>6</sup>R. Köhler, A. Tredicucci, F. Beltram, H. E. Beere, E. H. Linfield, A. G. Davies, D. A. Ritchie, R. C. Iotti, and F. Rossi, *Nature (London)* **417**, 156 (2002).
- <sup>7</sup>See a review, B. S. Williams, *Nat. Photonics* **1**, 517 (2007).
- <sup>8</sup>A. L. Betz, R. T. Boreiko, B. S. Williams, S. Kumar, and Q. Hu, *Opt. Lett.* **30**, 1837 (2005).
- <sup>9</sup>A. Baryshev, J. N. Hovenier, A. J. L. Adam, I. Kašalynas, J. R. Gao, T. O. Klaassen, B. S. Williams, S. Kumar, Q. Hu, and J. L. Reno, *Appl. Phys. Lett.* **89**, 031115 (2006).
- <sup>10</sup>J. R. Gao, J. N. Hovenier, Z. Q. Yang, J. J. A. Baselmans, A. Baryshev, M. Hajenius, T. M. Klapwijk, A. J. L. Adam, T. O. Klaassen, B. S. Williams, S. Kumar, Q. Hu, and J. L. Reno, *Appl. Phys. Lett.* **86**, 244104 (2005).
- <sup>11</sup>H.-W. Hübers, S. G. Pavlov, A. D. Semenov, R. Köhler, L. Mahler, A. Tredicucci, H. E. Beere, D. A. Ritchie, and E. H. Linfield, *Opt. Express* **13**, 5890 (2005).
- <sup>12</sup>M. Hajenius, P. Khosropanah, J. N. Hovenier, J. R. Gao, T. M. Klapwijk, S. Barbieri, S. Dhillon, P. Filloux, C. Sirtori, D. A. Ritchie, and H. E. Beere, *Opt. Lett.* **33**, 312 (2008).
- <sup>13</sup>L. Mahler, R. Köhler, A. Tredicucci, F. Beltram, H. E. Beere, E. H. Linfield, D. A. Ritchie, and A. G. Davies, *Appl. Phys. Lett.* **84**, 5446 (2004).
- <sup>14</sup>P. Khosropanah, J. R. Gao, W. M. Laauwen, M. Hajenius, and T. M. Klapwijk, *Appl. Phys. Lett.* **91**, 221111 (2007).
- <sup>15</sup>J. Faist, M. Beck, T. Aellen, and E. Gini, *Appl. Phys. Lett.* **78**, 147 (2001).
- <sup>16</sup>L. Ajili, J. Faist, H. Beere, D. Ritchie, G. Davies, and E. Linfield, *Electron. Lett.* **41**, 419 (2005).
- <sup>17</sup>A standard film provided by Moscow State Pedagogical University, Moscow, Russia.
- <sup>18</sup>For details of the NbN film on Si substrate, see J. R. Gao, M. Hajenius, F. D. Tichelaar, T. M. Klapwijk, B. Voronov, E. Grishin, G. Gol'tsman, C. A. Zorman, and M. Mehregany, *Appl. Phys. Lett.* **91**, 062504 (2007).
- <sup>19</sup>A. D. Semenov, H. Richter, H.-W. Hübers, B. Günther, A. Smirnov, K. S. Il'in, M. Siegel, and J. P. Karamarkovic, *IEEE Trans. Microwave Theory Tech.* **55**, 239 (2007).
- <sup>20</sup>The heat filter has an upper cutoff frequency of 5 THz and 0.22 dB loss at 3.42 THz and is made by QMC Ltd.
- <sup>21</sup>J. N. Hovenier, S. Paprotskiy, J. R. Gao, P. Khosropanah, T. M. Klapwijk, L. Ajili, M. A. Ines, and J. Faist, Proceedings of 18th International Symposium on Space Terahertz Technology, Pasadena, California, USA, 21–23 March 2007 (unpublished), p. 74.
- <sup>22</sup>M. I. Amanti (unpublished), available from <http://www.itqw07.leeds.ac.uk/Day1-Monday/T8.pdf>.
- <sup>23</sup>A. J. L. Adam, I. Kašalynas, J. N. Hovenier, T. O. Klaassen, J. R. Gao, E. E. Orlova, B. S. Williams, S. Kumar, Q. Hu, and J. L. Reno, *Appl. Phys. Lett.* **88**, 151105 (2006).
- <sup>24</sup>E. E. Orlova, J. N. Hovenier, T. O. Klaassen, I. Kašalynas, A. J. L. Adam, J. R. Gao, T. M. Klapwijk, B. S. Williams, S. Kumar, Q. Hu, and J. L. Reno, *Phys. Rev. Lett.* **96**, 173904 (2006).
- <sup>25</sup>A. R. Kerr, *IEEE Trans. Microwave Theory Tech.* **47**, 325 (1999).
- <sup>26</sup>The holding time can be kept as long as we need if we operate the cryostat as a flow cryostat.
- <sup>27</sup>J. J. A. Baselmans, A. Baryshev, S. F. Reker, M. Hajenius, J. R. Gao, T. M. Klapwijk, Yu. Vachtomin, S. Maslennikov, S. Antipov, B. Voronov, and G. Gol'tsman, *Appl. Phys. Lett.* **86**, 163503 (2005).
- <sup>28</sup>H.-W. Hübers, S. G. Pavlov, H. Richter, A. D. Semenov, L. Mahler, A. Tredicucci, H. E. Beere, and D. A. Ritchie, *Appl. Phys. Lett.* **89**, 061115 (2006).
- <sup>29</sup>W. Wild, Th. de Graauw, A. Baryshev, J. Baselmans, J. R. Gao, F. Helmich, B. D. Jackson, V. P. Koshelets, P. Roelfsema, N. D. Whyborn, and P. Yagoubov, Proceedings of 16th International Symposium on Space Terahertz Technology, Göteborg, Sweden, 2–4 May 2005 (unpublished), pp. 68–73.
- <sup>30</sup>Y. Irimajiri, T. Manabe, S. Ochiai, H. Masuko, T. Yamagami, Y. Saito, N. Izutsu, T. Kawasaki, M. Namiki, and I. Murata, *IEEE Geosci. Remote Sens. Lett.* **3**, 88 (2006).
- <sup>31</sup>S. S. Dhillon, J. Alton, S. Barbieri, A. de Rossi, M. Calligaro, H. E. Beere, E. H. Linfield, D. A. Ritchie, and C. Sirtori, *Appl. Phys. Lett.* **87**, 071107 (2005).
- <sup>32</sup>B. S. Williams, S. Kumar, and Q. Hu, *Opt. Express* **13**, 3331 (2005).